JOURNAL OF MECHANICAL ENGINEERING AND SCIENCES (JMES)
ISSN: 2289-4659 e-ISSN: 2231-8380
VOL.14, ISSUE 1, 6473 – 6487
DOI: https://doi.org/10.15282/jmes.14.1.2020.22.0507

ORIGINAL ARTICLE

Effects of geometric variations on buckling properties of carbon nanostructures: A finite element analysis

Farya Golesorkhie[1*] and Mani Navi[2]

[1] School of Engineering and built Environment, Griffith University, Gold Coast Campus, QLD 4222, Australia. Phone: +61422540364
[2] Faculty of Mechanical Engineering, Science and Research branch, Islamic Azad University, 1477893855, Tehran, Iran.

ABSTRACT – Critical Bucking Load (CBL) is one of the essential parameters to describe the mechanic stabilities of materials, e.g. the low-dimensional carbon nanostructures. While the CBL of pristine carbon nanotubes have been previously investigated using the quantum mechanics-based calculations, the effect of geometrical variation on the CBL of carbon nanomaterials is rarely reported since it need considerably large atomic models, which needs high computational cost. In this study, both the analytical and Finite Element (FE) methods were employed to systematically explore the impact of atomic vacancies, shapes and heterostructures on the CBLs of carbon nanomaterials with the acceptable computational cost. Our studies on the pristine CNTs first demonstrate the validity of the method we used. After that, the systems with mono-/bi-/tri-/pinole-vacancies either on nanocones, nanotube, linearly-joined nanotubes or angle-adjoined were simulated and analyzed. Our results reveal that the CBL values decrease with the increase of the aspect ratio of all considered nanomaterials. Based on the obtained results, the CBL of nanocone with the aspect ratio of 1, reduces significantly, from 50 nN to 10 nN when the aspect ratio is 3. The CBL of homogeneous, capped, and joint CNTs reduces to below 2 nN when the aspect ratio is above 14. The introduction of geometric variations can greatly affect the CBL values. The larger atomic vacancy has more serious impact on the CBLs. The most highlighted impact is for the pinhole vacancy where the CBL reduces to up to 70% of the original value. Our studies on linearly-joint and angle-joint carbon hybrids further demonstrate that the CBL can also be affected by the boundary conditions and joint structures of the hybrids.

ARTICLE HISTORY
Revised: 1st Nov 2019
Accepted: 7th Nov 2019

KEYWORDS
carbon nanostructures; finite element method; critical buckling load; geometric variation; aspect ratio.

INTRODUCTION

Carbon Nanotubes (CNTs) and their degenerated modifications including nanocones, capped CNTs, fullerene, Y-junctions, linearly-joined and angle-adjoined CNTs, are a class of promising low-dimensional materials used in the electronics, composites, and energy conversion areas, which performance are directly related to their mechanical properties and stabilities [1-16]. The buckling of nanomaterials under compression loading, is influenced by the physical height of the models, their axial symmetry, relative position to normal reference plane and their fixation mode. Buckling is an essential parameter often utilized to examine nanomaterials mechanical behaviors [7-11]. As such, the buckling of single- and multi-walled CNTs have been previously investigated. The buckling properties generally depend on the structural organization of the nanomaterial structures, which can be computationally analyzed using the quantum mechanics-based approaches [12,13]. In 2011, Feliciano et al. [14] conducted a Molecular Dynamics (MD) simulation to study the structural stability of CNTs with a single layer under the influence of aspect ratio. They studied the variation of bond angles and lengths to explore the underlying mechanism. Their analysis results revealed the fact that any specific change in aspect ratio can lead to distinct buckling modes in the tube models. Silvestre et al. [15] also examined the influence of aspect ratio on the buckling property of Single-Walled CNTs (SWCNTs) by simulating Donnell and Sanders shell models. They found that the Sanders shell theory is far more correct in investigating the buckling response of CNTs in comparison with the Donnell shell approach. Later, Li et al. [8] investigated the stability of CNT intramolecular junctions by applying the MD approach. They carried out their analysis at a finite temperature and observed that the structural strength of the intramolecular junction transfers from shell buckling to column buckling with increase in the tube length.

Despite the comprehensive investigations regarding the structural stability of perfect CNTs, the mechanical response of defective, degenerated low-dimensional systems has not been systematically explored. This is largely ascribed to the large size of required atomic models to simulate the systems with geometric deviation, which demand high computational cost [16]. However, investigating the mechanical response of the imperfect and atomically modified low-dimensional configurations is crucially important since these geometric deviations are closer to those found in practice applications. To this end, their characteristics should be addressed.

To efficiently reduce computational time and lowers the demand for resources while rendering highly plausible simulation results, the crystal-based Finite Element Method (FEM) have been utilized to investigate mechanical properties

*CORRESPONDING AUTHOR | Farya Golesorkhie | ✉ Farya.golesorkhie@griffithuni.edu.au

and deformation-induced crystallographic structures. Crystal-based FEM is a versatile continuum mechanics approach, which can be used for solving both elastic-plastic and purely elastic problems of multi-body systems and complex CNTs (> 1.0 x 10^5 atoms) model structures [4, 17-21]. In 2008, Yao et al. [22] explored the buckling response of CNTs with different layers by applying a modified FEM. In 2013, Hollerer and Celigoj [23] conducted an investigation to study the buckling response of CNTs by applying a mixed atomistic and continuum model and performed the numerical analysis of CNTs using FEM. Their simulation results demonstrate that FEM is s an efficient alternative method to investigate the mechanical response of pristine CNTs.

Although the properties of homogeneous and defect-free CNTs have been widely studied, the mechanical properties of the other CNT derivatives, e.g. nanocones, capped and joint CNTs have not been explored. These carbon nanostructures are considered so applicable in science and engineering and much effort should be put to obtain their mechanical characteristics. Furthermore, the influence of the structural defects on the mechanical behavior of such low-dimensional structures needs to be explored and investigated as simulating the defected material models makes them very close to the ones found in reality.

In this study, the FEM is employed to investigate the effect of geometric variations on the buckling property of low-dimensional carbon nanomaterials. We first calculated the critical buckling load (CBL) characteristics of carbon nanocone, homogeneous CNTs and linearly-joined and angle-adjoined CNTs under axial loading. Our results confirm the significant relevance to CBL to the aspect ratios of nanomaterials. After that, we investigate the impact of a wide range of atomic vacancies, e.g. mono-/di-/tri-/pinhole vacancies, on the CBL of nanostructures with different boundary conditions. Our FEM results evidence that the mechanical characteristics of carbon nanomaterials is greatly influenced by their axial symmetry, positions of vacancies in their structure, and boundary conditions.

MODELLING DETAILS

The carbon nanostructures were created by using a two-dimensional (2D) single layer graphene sheet, as illustrated in Figure 1(a). The nanocone was built through wrapping a cone sheet and can be defined with regard to its height and also its disclination angle, which are represented as 20 Å and 180°, respectively. The homogeneous CNTs were modeled by rolling a single layer sheet of graphene, and categorized as zigzag-, armchair-, or chiral- CNTs, which are defined in terms of their chiral vector ($\vec{C}_h$) and chiral angles (θ). The $\vec{C}_h$ is defined by $\vec{C}_h = n\vec{a}_1 + m\vec{a}_2$, where $\vec{a}_1$ and $\vec{a}_2$ are unit vectors and two integers, *n* and *m* are steps along the unit vectors (see Figure 1(b)). The diameter of the CNTs is then calculated based on the following equation:

$$d_{\mathrm{CNT}} = a_0\sqrt{(m^2 + mn + n^2)/\pi} \tag{1}$$

where $a_0 = \sqrt{3}b$. And *b* is the length of the C-C bond of 0.142 nm [24].The linearly-joined CNTs were set up through the combination of a (5,5) thinner armchair CNT on the top of a (10,10) wider armchair CNT. And the angle-adjoined CNTs were established through the combination of a (10,0) zigzag tube on the top of an (5,5) armchair tube. All the geometric deviations were introduced and applied using a custom code in MATLAB® (MathWorks, MA, USA) to the original defect-free, ideal models at 1.0 at. % to the total number of atoms in the system. Since the atomic defects can be introduced to the structures of the nanoparticles in different sizes and shapes in experimental conditions, four types of atomic vacancies, including mono-/di-/tri-/pinhole-vacancies, were studied within the three regions: i.e. upper region, middle (or junction region in the case of hybrid CNTs), and lower region of the nanostructures, as illustrated in Figure 2. The spatial coordinates of atoms and their bonding vectors for all low-dimensional models were generated using Nanotube Modeler® software package (©JCrystalSoft) and imported to a commercial FEM package Marc® (MSC Software Corporation, CA, USA). This package will then simulate and run the buckling condition of the nanomaterial models and finally the computational value of CBL of the nanostructures can be obtained.

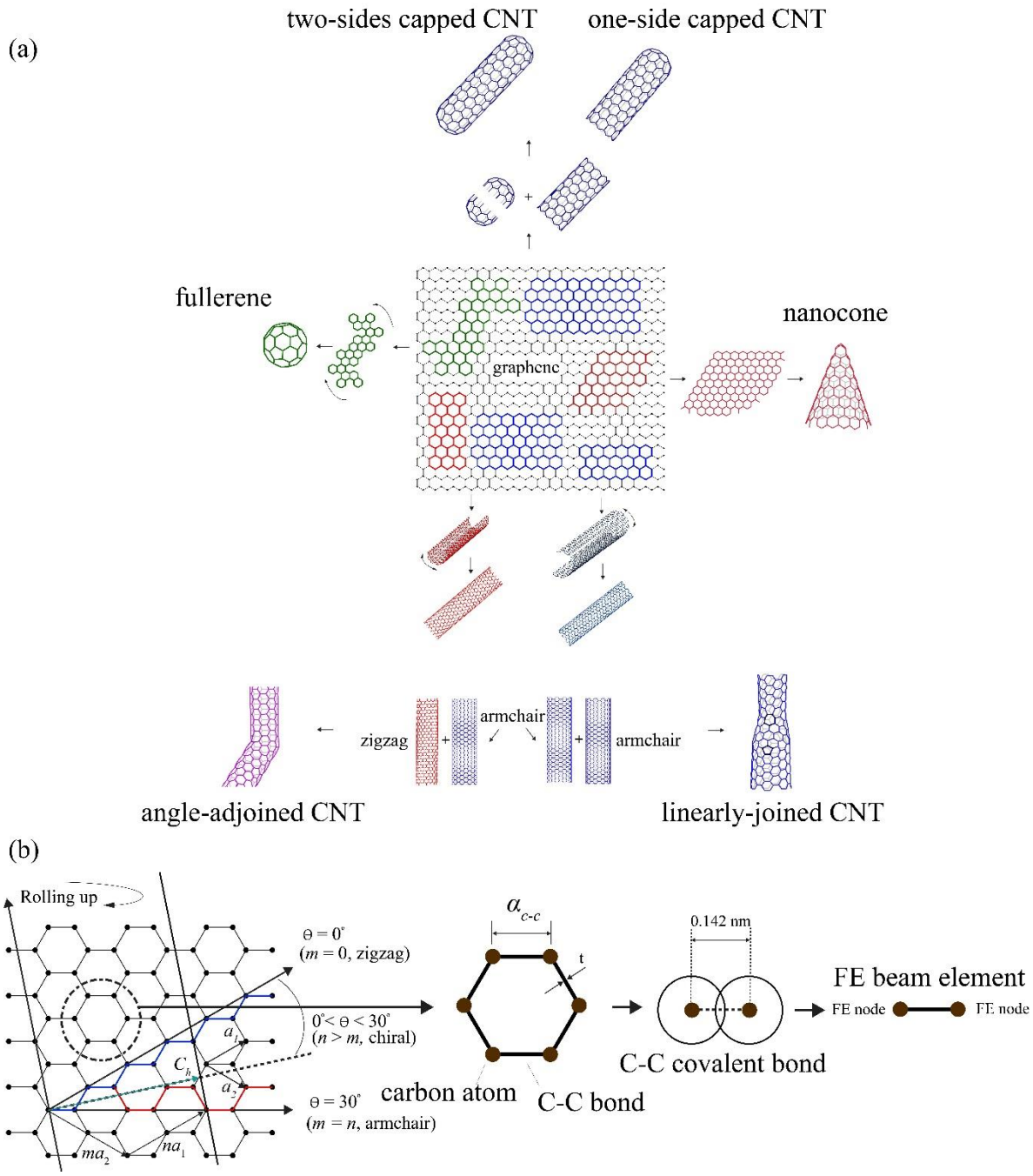

Figure 1. Geometry of carbon nanostructures [21].

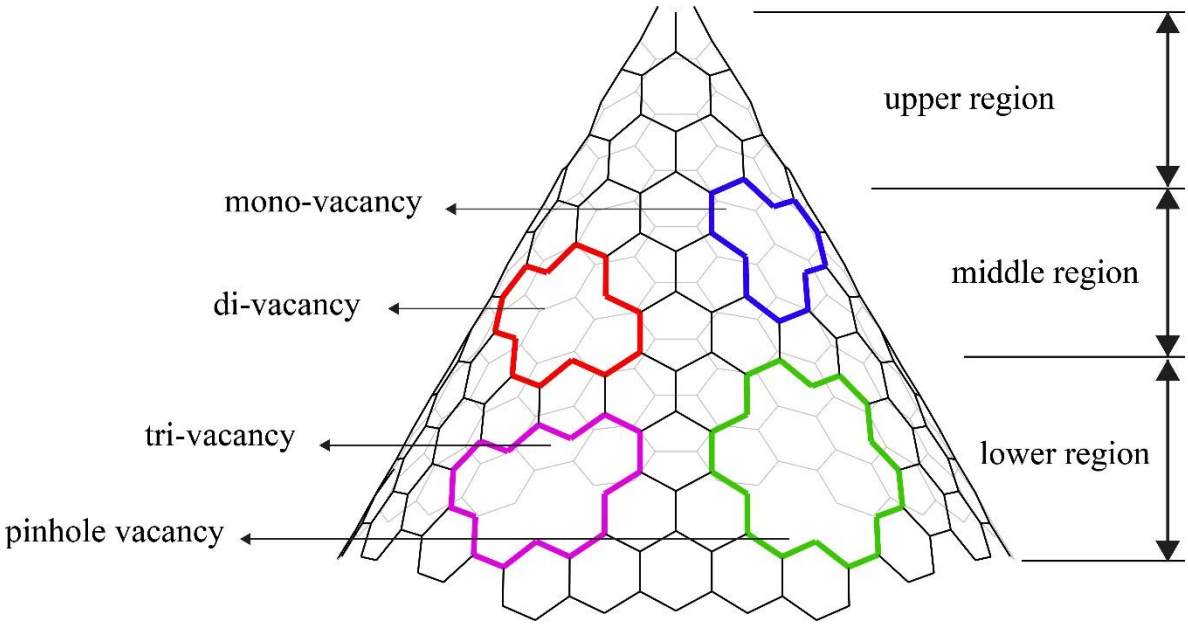

Figure 2. Different types of vacant sites and location of these impurities on the structure of the nanocone.

Our modeling method follows the idea first proposed in [25] where the theory of classical structural mechanics was extended into the modeling of CNTs: In a carbon nanotube, carbon atoms are bonded together by covalent bonds which have their characteristic lengths and angles in a three-dimensional space. It was then assumed that CNTs, when subjected to loading, behave like space-frame configurations. Thus, the bonds between carbon atoms are considered as connecting load-carrying generalized beam members, while the carbon atoms act as joints of the members. The gathered data transferred to the finite element package, where C–C bonds were modeled as circular beam elements [26]. These elements are based on Timoshenko's beam theory with shear deformation effects included and the ability of torsional deformations around the longitudinal axis.

The critical buckling response of a system naturally depends on the overall geometry, boundary condition and basic configuration of the system. Analytically, the CBL of a structure (P_{cr}) in its simplest form can be defined by the equation [27]:

$$P_{cr} = \frac{n^2\pi^2 EI}{(Kl)^2} \tag{2}$$

where K is the effective length constant, E is the Young's modulus of the structure, l is the total length of the model, n is the buckling mode and I is the second moment of area. In our calculations, $K = 2$ used for the cantilever-type systems and an n of 1 used for the initial simulation of the first buckling mode. Since, homogeneous CNTs can be viewed as a hollow cylinder, therefore, the following equation can be used to define the second moment of area:

$$I = \pi[(d+t)^4 - (d+4)^4]/64 \tag{3}$$

where d is the diameter of the CNT and t is represented as the thickness of the CNTs shell. Due to conducting the buckling test, the boundary condition carried out within this study is the fixed-free condition where the upper end of the structure is subjected to a compressive load. This analysis is set to a static calculation where the critical buckling load is obtained, providing the structure mechanical stability with respect to compressive loads.

Here, the thickness values of the CNTs and their derivations are same as the interlayer spacing of graphite (0.34 nm), which in detail is discussed in [25, 28]. The l values can be determined based on the configurations of carbon materials. The linearly-joined and angle-adjoined CNTs are built by joining two homogeneous CNTs together along their axes of symmetry and introduce the Stone-Wales defects in their configurations. The length of the linearly-joined or angle-adjoined CNT (l) is defined by the equation:

$$l = l_t + l_j + l_w \tag{4}$$

where l_t, l_j, and l_w are the lengths of the thinner CNT, the junction region, and the wider CNTs, respectively. As aforementioned, the chirality of the connected CNTs for linearly-joined CNT was (5,5) and (10,10) armchair tube. For the case of angle-adjoined hybrids, a (5,5) armchair CNT is joined with a (10,0) zigzag CNT. The l_j is determined by the diameters of the connected CNTs:

$$l_j = \frac{\sqrt{3}}{2}\pi(d_w - d_t) \tag{5}$$

where d_w *and* d_t are the diameters of the wider and the thinner CNTs, respectively. The diameter of the junction region is varied based on the chirality of the corresponding connected tubes. Since there is no particular geometric pattern for the junction region, the diameter of the junction region ($\bar{d}_j$) is defined as the average value of d_w *and* d_t. And finally, the aspect ratio (η) of the connected hybrids can be calculated by:

$$\eta = \frac{l}{\bar{d}} \tag{6}$$

The stiffness characteristics of the beam for elongation, bending and torsion were obtained as function of three force field constants for stretching (k_r), bond angle bending (k_θ) and torsion (k_φ), as illustrated in Figure 1(c). Since there is no available classical test or geometric derivations to define the characteristics of one dimensional (1D) carbon beam element, we assume that the values of material properties for the equivalent beam element are same as previously reported ones (k_r = 651.97 nN/nm, k_θ = 0.8758 nN·nm/rad^2, and k_φ = 0.27 nN·nm/rad^2) [25, 28, 29]. As such, the 1D carbon bonds have the interatomic characteristics as listed in Table 1, which were then imported to the FE software for processing [30, 31].

Table 1. Geometric characteristics of one-dimensional carbon-carbon bonds.

Young's modulus $E = \frac{k_r^2 b}{4\pi k_\theta}$	**Bond radius** $R_b = 2\sqrt{\frac{k_\theta}{k_r}}$	**Second moment of area** $I_{xx} = I_{yy} = \frac{\pi R_b^4}{4}$	**C − C bond cross − section area** $A_{C-C} = \pi R_b^2$
5.484×10^{-6} N/nm^2	0.0733 nm	2.2661×10^{-5} nm^4	0.0169 nm^2

The FE simulation procedure of this study is shown in the following block diagram (Figure 3).

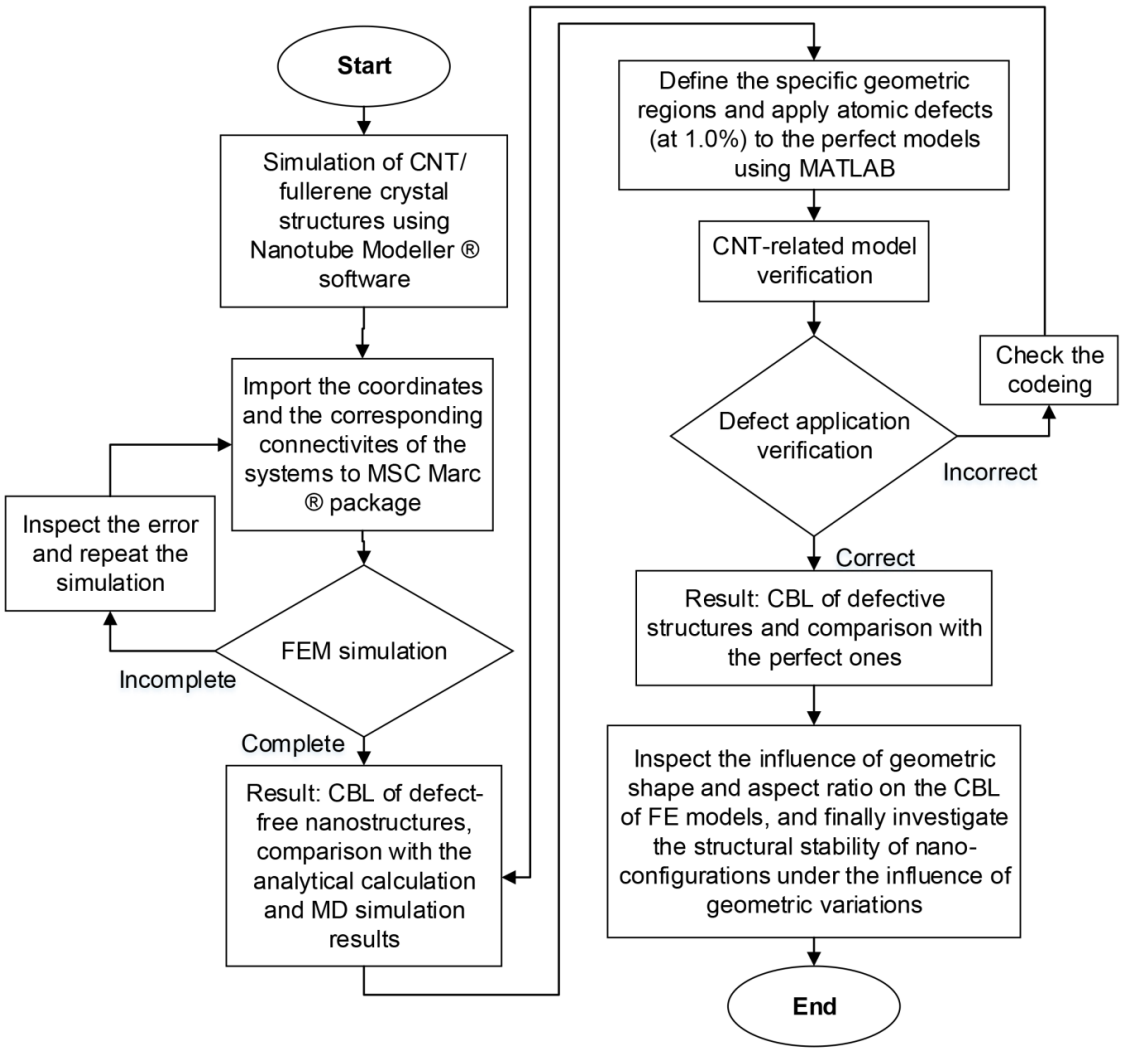

Figure 3. Block diagram indicating the procedure for investigation of the structural stability of defect-free, atomically modified carbon nanostructures.

RESULTS AND DISCUSSION

Validation of the Method

The CBL of homogeneous CNT was first calculated here to validate the FEM and parameters we employed in this study. Figure 4 illustrates an example to show the buckling mode shape of a linearly joined CNT with the parallel longitudinal axis under a compressive load. Mehralian et al. found that the CBL of a (10,10) armchair CNTs with the aspect ratio of $l/d > 9$ in their research was within the range of 20 to 25 nN using the MD simulation [32]. Similarly, Poelma et al. applied the same MD simulation to evaluate the CBL of different CNTs versus the CNT length to diameter ratio [33]. For the case of $l/d = 12$, the value of CBL was around 25 nN. In this study, the CBL value of the homogenous (10,10) armchair CNT with the aspect ratio of 12 is 24.01 nN, which is in good agreement with previous MD results [32]. It, therefore, demonstrate that the method and parameters we employed here is valid. A comparison between the obtained results within this study and the one evaluated in literature is presented in Table 2.

Table 2. The CBL of homogenous CNTs obtained in this study and the ones evaluated in the literature.

Author	Material	Method	Aspect ratio [*l*/*d*]	CBL [*nN*]
Mehralian et al. [32]	Armchair CNT	MD	More than 9	25
Poelma et al. [33]	Armchair CNT	MD	12	25
Present	Armchair CNT	FEM	12	24

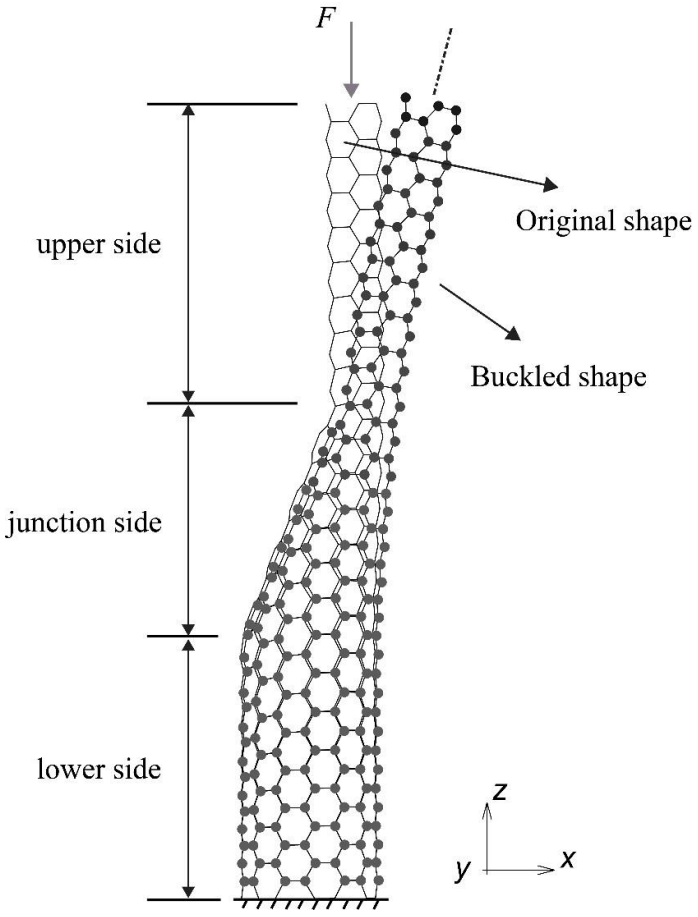

Figure 4. Critical buckling mode shape of a linearly-joined CNT under compression loading.

Influence of Shape and Aspect Ratio

Next, the buckling responses of carbon nanostructures under the impact of their shape and aspect ratio (l/d) were evaluated, as shown in Figure 5. Here, the ratio of height to the base diameter was considered for the case of nanocones. And the aspect ratios of the hybrid CNTs are calculated by the Equation. (6). It can be found that the CBL decrease with the increase of aspect ratio for all the considered carbon nanostructures. While the converged CBL values in terms to the aspect ratios for nanocone, joint CNTs and homogenous CNTs are similar, which is less than 20 nN, the structural strength of these nanostructures in response to aspect ratio is different. Figure 5 demonstrates the great influence of aspect ratio

on the CBL of the nanocone, hybrid CNTs, homogeneous CNTs without or with caps. As evidenced by Figure 5(a), there is an extensive reduction in the structural stability of nanocones with the increase of the aspect ratio. It is reducing from the aspect ratio of 1 at 50 nN to approximately 10 nN with the aspect ratio of 3, which is a significant drop. Increasing the aspect ratio leads to an enormous reduction of the CBL for both linearly-joined and angle-adjoined CNTs. However, as shown in Figure 5(b), in the case of the angle-joined CNT with the armchair tube fixed, this reduction is too moderate in comparison with the other boundary conditions. It indicates that the shape of angle-joined CNT can greatly affect their CBL and stabilities. In addition, it suggests that the unlike the other boundary condition, the small rates of aspect ratio do not increase the CBL value to the higher domains. To be more precise, the CBL of the joint CNT with the wider tube fixed reduces from 70 nN to less than 10 nN when the aspect ratio changes from 5 to 15. The joint CNT with the thinner tube fixed however, keeps moderately reducing its CBL from 5 to almost 1 nN within that phase. As a comparison, homogenous, one-side, and two-side capped (10,10) armchair CNTs react almost identically to a change in aspect ratio (see Figure 5(c), which indicates that the boundary configuration of CNTs has slight influence on their stability. It can be noticed the CBL of homogeneous, one-side capped and two-sides capped CNTs reduce from approximately 90 nN to less than 20 nN when the aspect ratio is changing from 5 to 15.

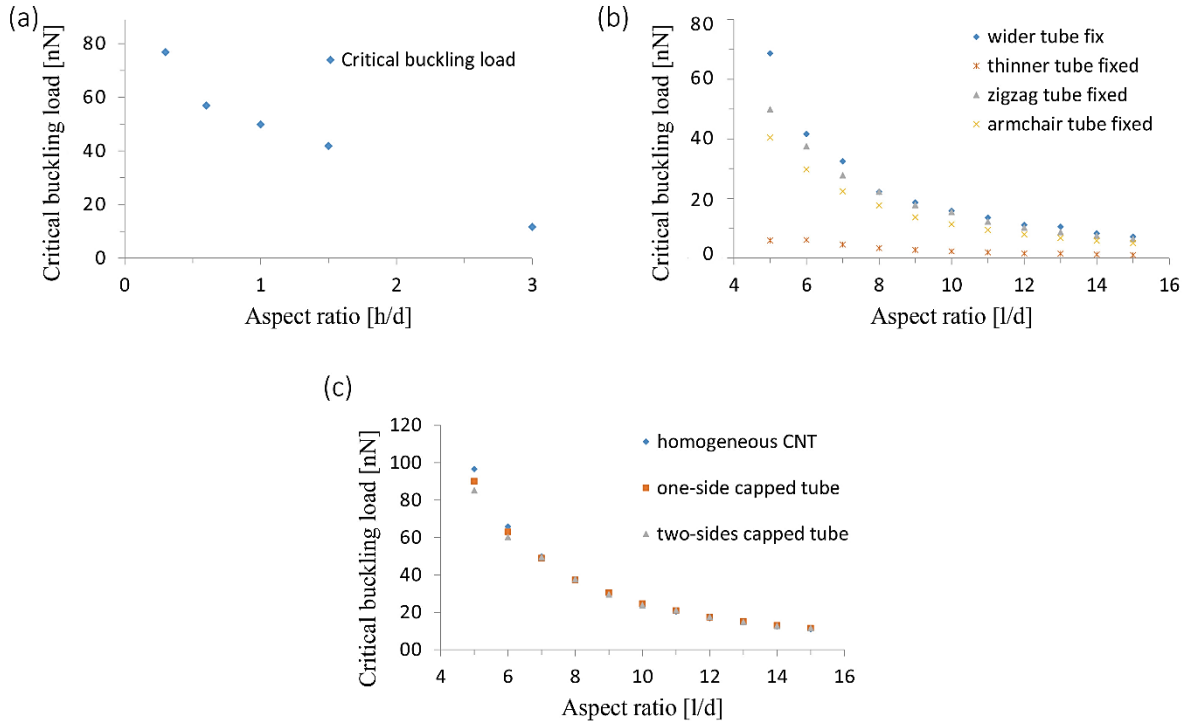

Figure 5. Change of critical buckling load of (a) nanocone, (b) linearly-joined and angle-adjoined CNT hybrids, and (c) homogenous, one-side capped and two-side capped CNTs under the influence of aspect ratio.

Effect of Vacancy

Four different types of vacancies, including mono-/di-tri-/pinhole-vacancies, with 1% of the total carbon atoms were introduced to understand the vacancy effect on the CBL, as illustrated in Figure 2. The aim of dividing the nanostructures into different regions is to identify the most critical regions of the material models on CBL after the introduction of vacant sites. Our results show that the presence of vacancies reduces the CBL and ultimately lessens the structural strength of the nano-configurations in all cases of boundary conditions. The CBL value of for a defect-free nanocones configuration is 35.92 nN with the aspect ratio of 1.5, which was used as a reference to analyse the effect of vacancies. As shown in Figure 6, the upper region of the nanocone is the most critical part. Any type of atomic vacancies in this region can lead to a high reduction in the CBL of the model. Moreover, the change of CBL increase with the increase of the size of vacancies. The introduction of mono-vacancies decreases the CBL by 6.26 %. The change of CBL increase to 26.54 % when there is a pinhole-vacancy in the upper region. In contrast, the middle and lower regions of the nanocone are not sensitive to the vacant sites to the critical buckling load with the change of CBL less than 1% for all the considered defective configurations. It can be ascribed to the fact that the middle and lower regions consist of much more atoms comparing the upper region and the existence of atomic defects seems to be less critical for those regions.

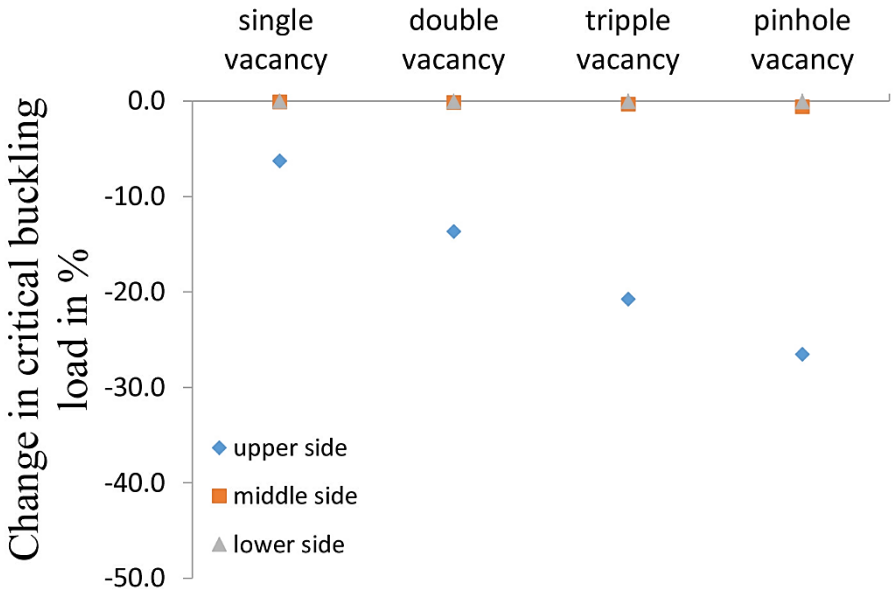

Figure 6. Change in critical buckling load in % for vacancy defected nanocone with different defected regions.

For the case of defect free structures of homogenous, one-side capped, and two-side capped CNTs, the values of CBL were obtained at 24.01 nN, 26.64 nN, and 28.54 nN, respectively, with the aspect ratio of 12, which have been used as the reference to understand the vacancy effect. As shown in Figure 7, the CBL of all three nanotubes, homogeneous, one-side capped and two-side capped CNTs, drop considerably after the introduction of vacancies, especially in the case of pinhole vacancy. The most instability occurs when the microscopic defects were at the lower region of the tubes, which is different from that observed in nanocone.

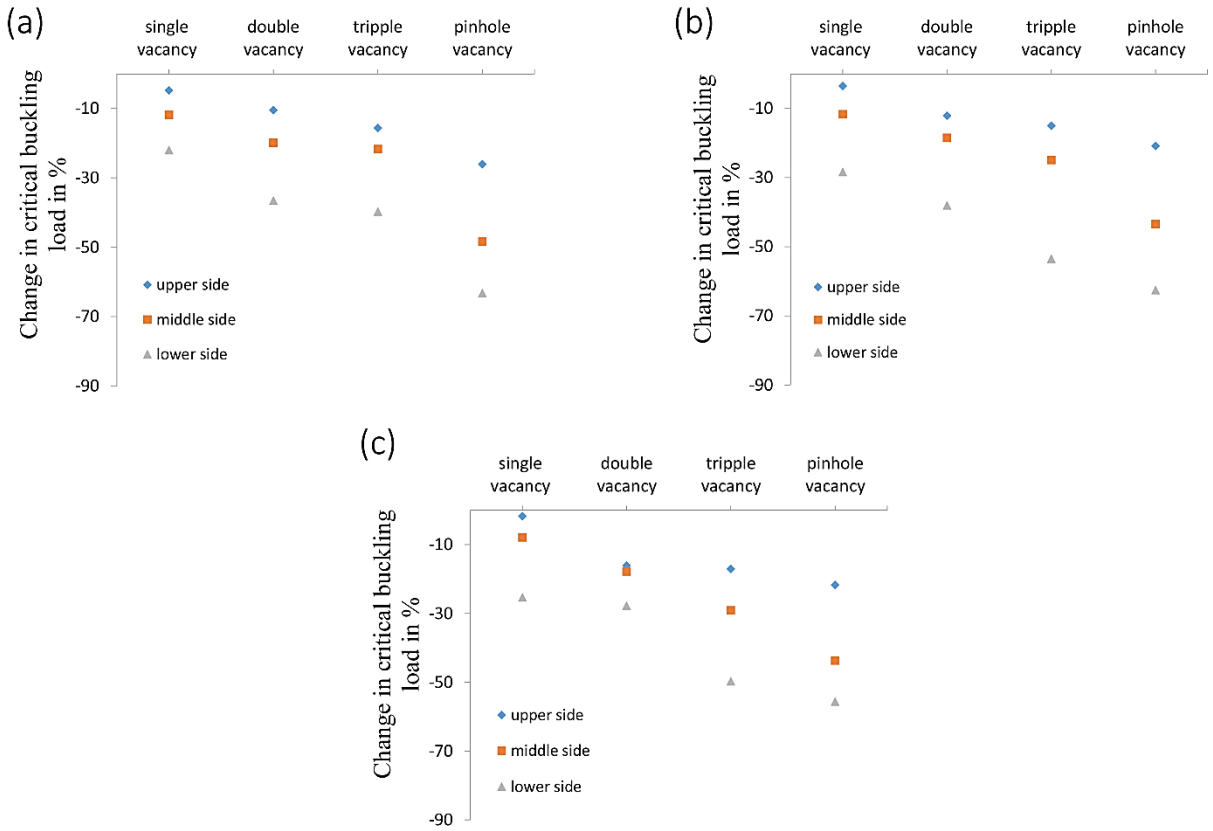

Figure 7. Change in critical buckling load in % for vacancy defected (a) homogeneous, (b) one-side capped and (c) two-side capped CNTs with different impurity regions.

In the case of linearly-joined CNTs, two different boundary conditions were considered with the fixed the wider or thinner tube. The corresponding reference CBL values based on these defect free structures are 16.63 nN and 2.41 nN, respectively, with the aspect ratio of 14. As shown in Figure 8(a), the greatest reduction in the CBL occurs when the vacancy is at the upper region of the hybrid junction if the wider tube is fixed. On the other hand, the critical region is the thinner tube in the case of the thinner tube being fixed since the change of the stability is considerably larger when the vacancies locate at the thinner tube of the hybrid junction, as demonstrated in Figure 8(b). If the two connecting nanotubes are not of the same type, the created junction hybrid will have a bending junction. In this case, two different boundary conditions could be considered with the fixed zigzag or the armchair tube. The reference CBL values from for the corresponding defect free structures were reported as 15.01 nN and 11.73 nN, respectively, with the aspect ratio of 14. However, the significant change occurred when the vacancy was applied to the lower region with the fixed zigzag CNT boundary (see Figure 8(c)). Surprisingly, the largest reduction occurs when the vacancies are at the junction region of the bending hybrid with the fixed armchair CNT boundary, as shown in Figure 8(d).

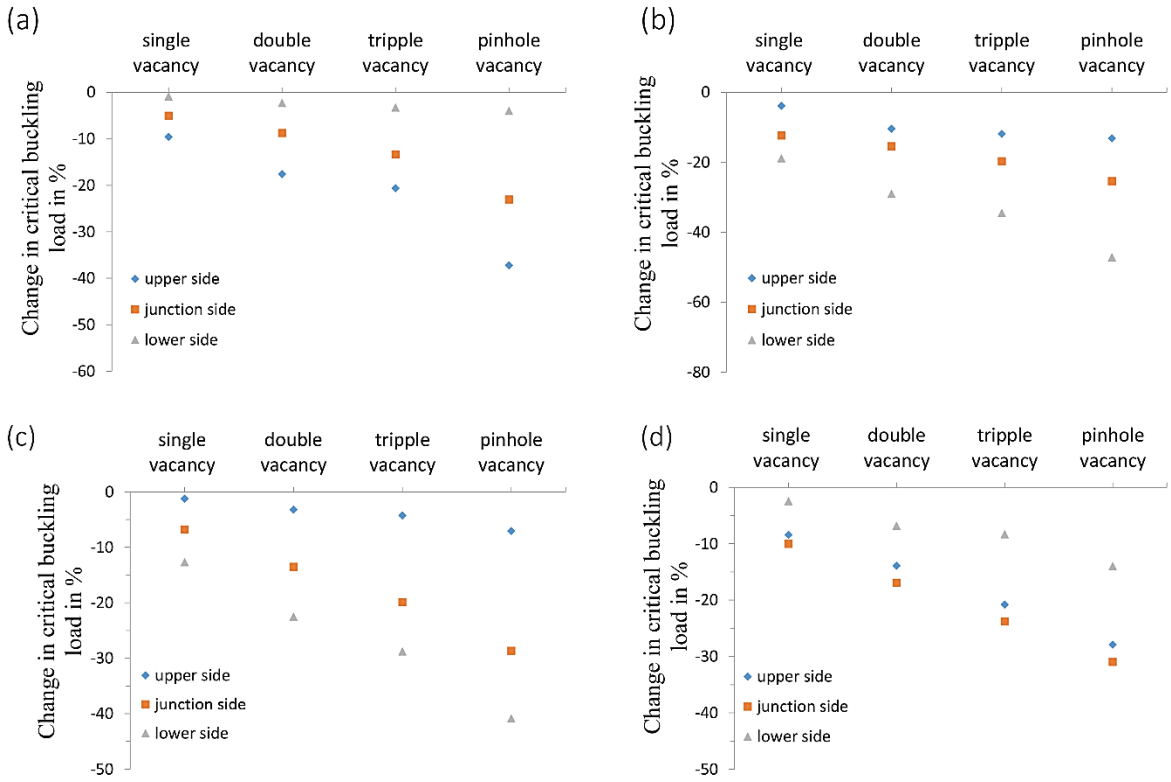

Figure 8. Change in critical buckling load in % for linearly-joined CNTs with (a) wider tube fix and (b) thinner tube fix, and for angle-adjoined CNTs with (c) zigzag tube fix and (d) armchair tube fix boundary conditions.

DISCUSSION

Since the geometric deviations can cause different impact on the CBL of the nanostructures, we can analyze the buckling response of asymmetric nanostructures including linearly-joined and angle-adjoined CNTs, one-side capped cylindrical fullerene, and nanocone to emphasize the sensitivity of the low-dimensional asymmetric systems in terms of the regions of imperfections. The FE analysis results indicate that, the values of CBL significantly vary in terms to the location of the structural defects. As an instance, based on Figure 9(a), it was revealed that the value of CBL of a nanocone which is defected by 1% of single vacancy in the upper region, equals to its CBL when subjected to 7% single vacancy defect in the lower region of the structure. Thus, it demonstrates that the upper region of the nanocone is structurally more instable in comparison with the lower region of the nanocone. This is becasue the more atoms is in the lower region of the nanocone. Afterwards, we explored the influence of different types of atomic defect on the significant regions of the asymmetric nanostructures. As shown in Figure 9(b), the CBL of the nanocone with 0.4% mono-vacancy at the upper region is similar as that with 1% pinhole vacancy at the lower region. It suggests that the pinhole vacancy has the major influence on the structural stability of the carbon-based nanostructures since the number of extracted nodes and their corresponding beam elements is more than the number of those extracted by the other types of vacancy defects.

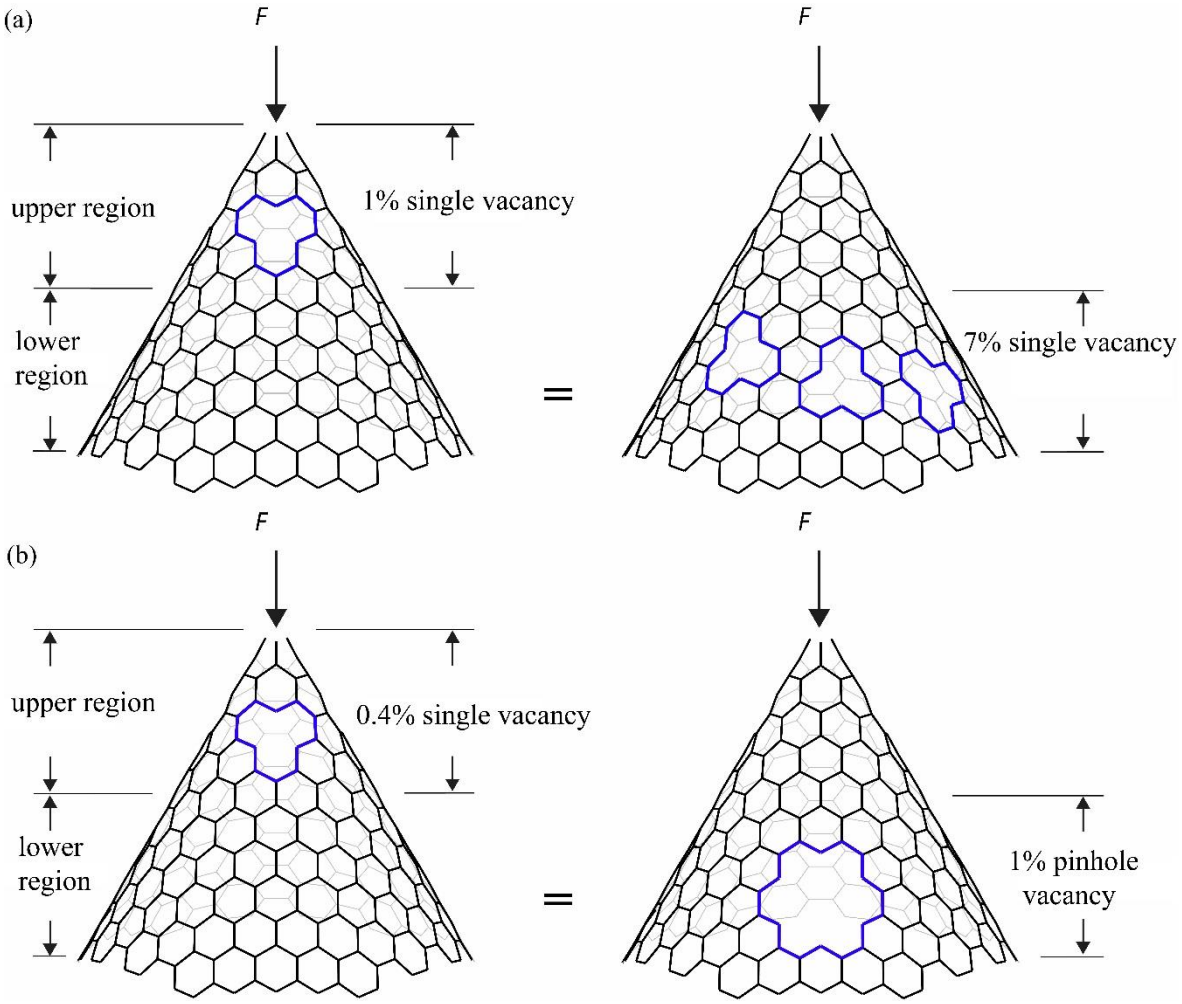

Figure 9. The simulation of buckling analysis of nanocone under the influence of atomic defects.

On the contrary, the CBL value with 1% of the mono-vacancy in the upper region is same as that with only 0.5% of mono-vacancy in its lower region, as illustrated in Figure 10(a). Figure 10(b) depicts that an asymmetric one-side capped CNT has just the same value of CBL when subjected to 1% single vacancy defect in the lower region and 0.6% double vacancy defect in the upper region of the structure. It indicates that the stability of the upper region of CNTs is more sensitive to the vacancies, which is different from the trend observed in the nanocone. This difference is caused by the different shapes of nanomaterials. In the CNT, the atom numbers are same in the different regions. Considering that the external force is directly exert on the upper region, the stability of the upper region, therefore, is lower under this condition.

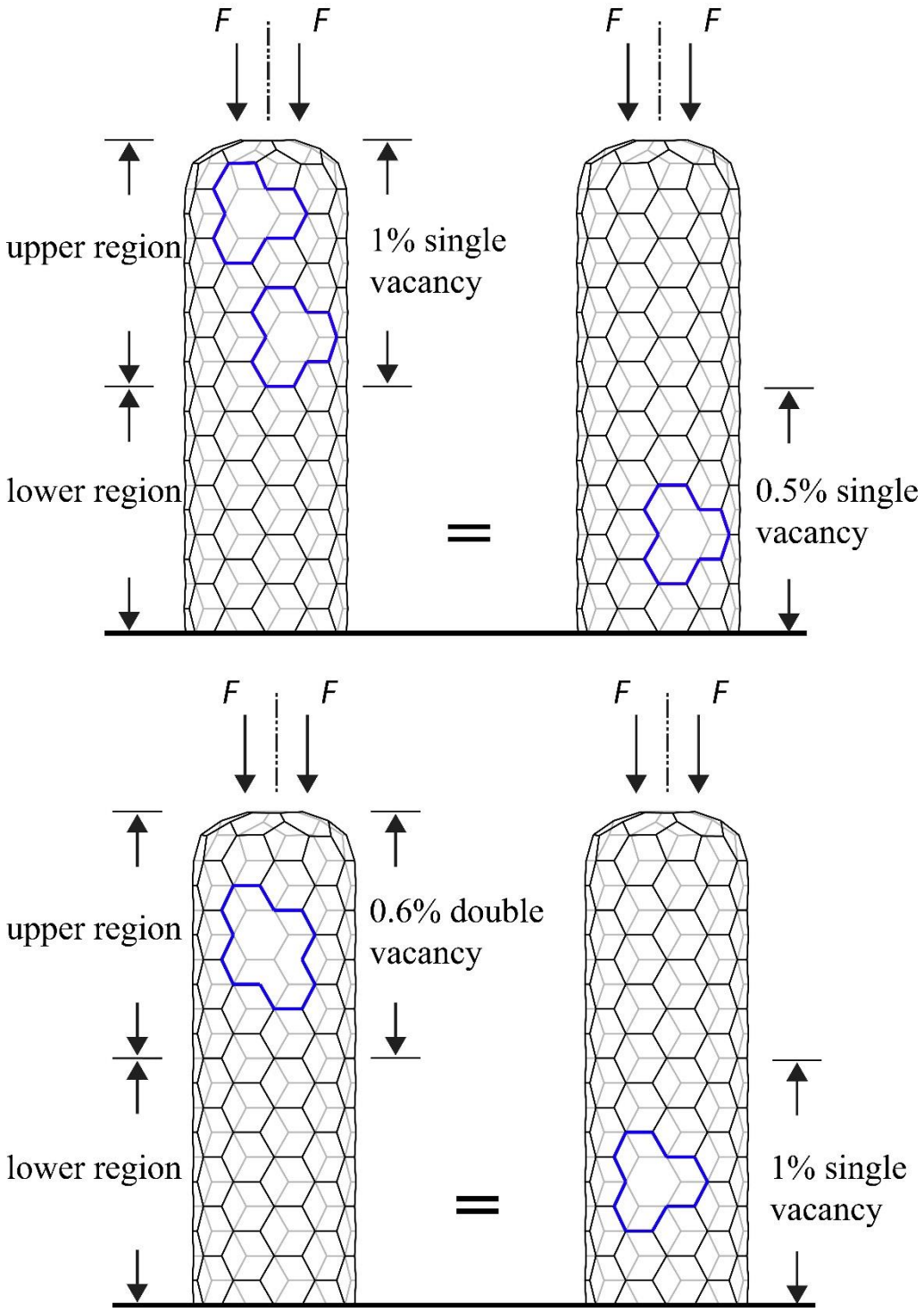

Figure 10. The simulation of buckling analysis of one-side capped CNT under the influence of atomic defects.

This analysis becomes more complex when hybrid CNTs are investigated based on their particular structures. As shown in Figure 11(a), FE results indicate that the CBL value are same when the concentrations of mono-vacancy in the upper region (thinner CNT), the connecting junction, and the lower region (wider CNT) are 1%, 1.5%, and 3.5%, respectively, in a linearly-joined CNT. And 1% of mono-vacancy defect in the lower region of a linearly-joined CNT (the wider CNT fixed) has the same stability of these with 0.4% of bi-vacancy defects and 0.25% of tri-vacancy defect is introduced in the connecting region and the upper region (thinner CNT), as shown in Figure 11(b).

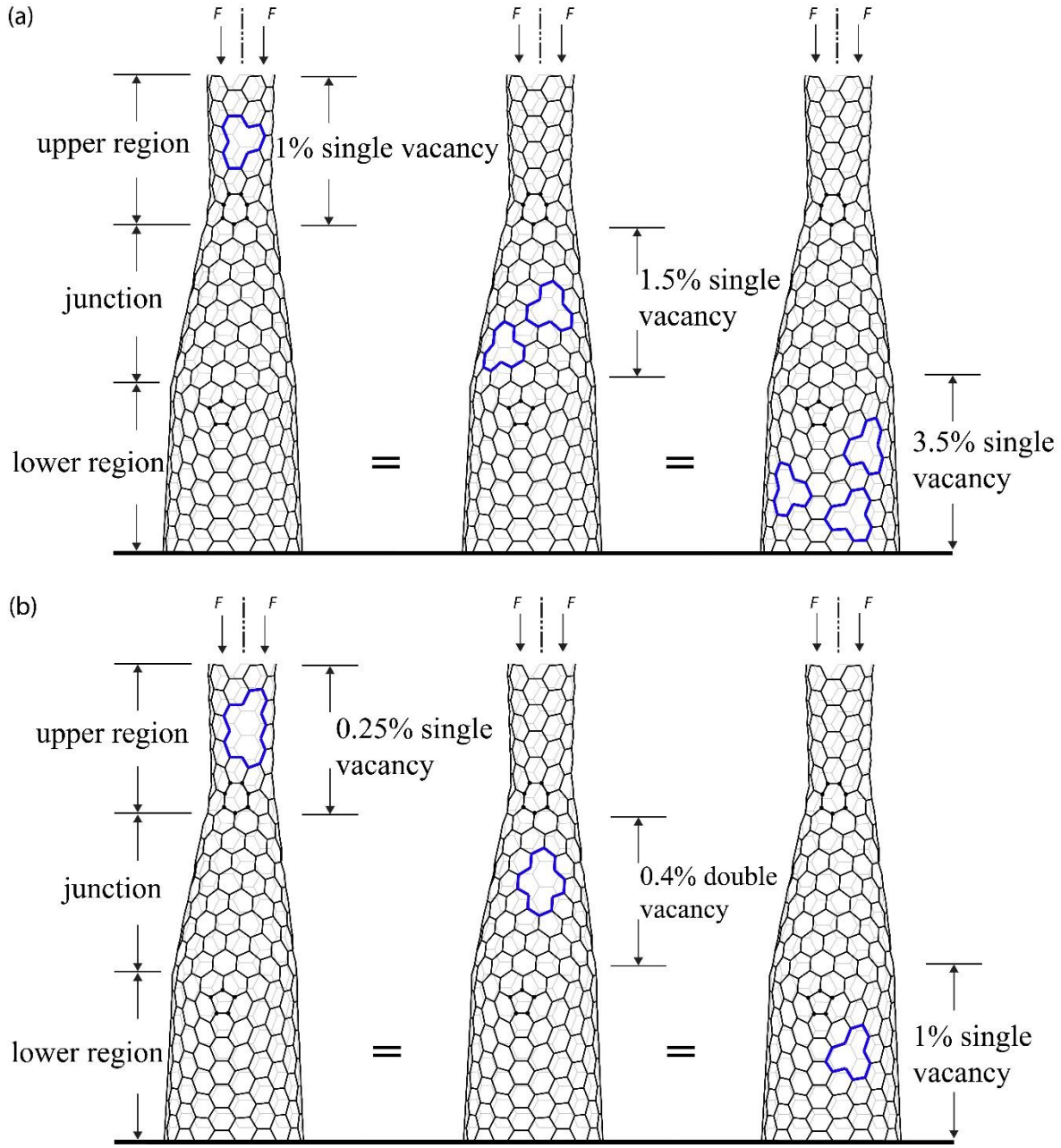

Figure 11. The simulation of buckling analysis of linearly-joined CNT under the influence of atomic defects.

The buckling analysis on the asymmetric angle-adjoined CNTs is also significant (see Figure 12). According to the FE analysis results, the introduction of 1% of mono-vacancy to the upper region (zigzag CNT) of an angle-adjoined CNT has the similar effect as that after the introduction of 1.2% and 2.5% of the same defect to the connecting region and lower region (armchair CNT), respectively (see Figure 12(a)). Interestingly, the value of CBL is the same when 1%, 0.6% and 0.3% of mono-vacancy, bi-vacancy, and tri-vacancy are introduced to the lower connecting, and upper regions of the CNT hybrid, respectively (as depicted in Figure 12(b)).

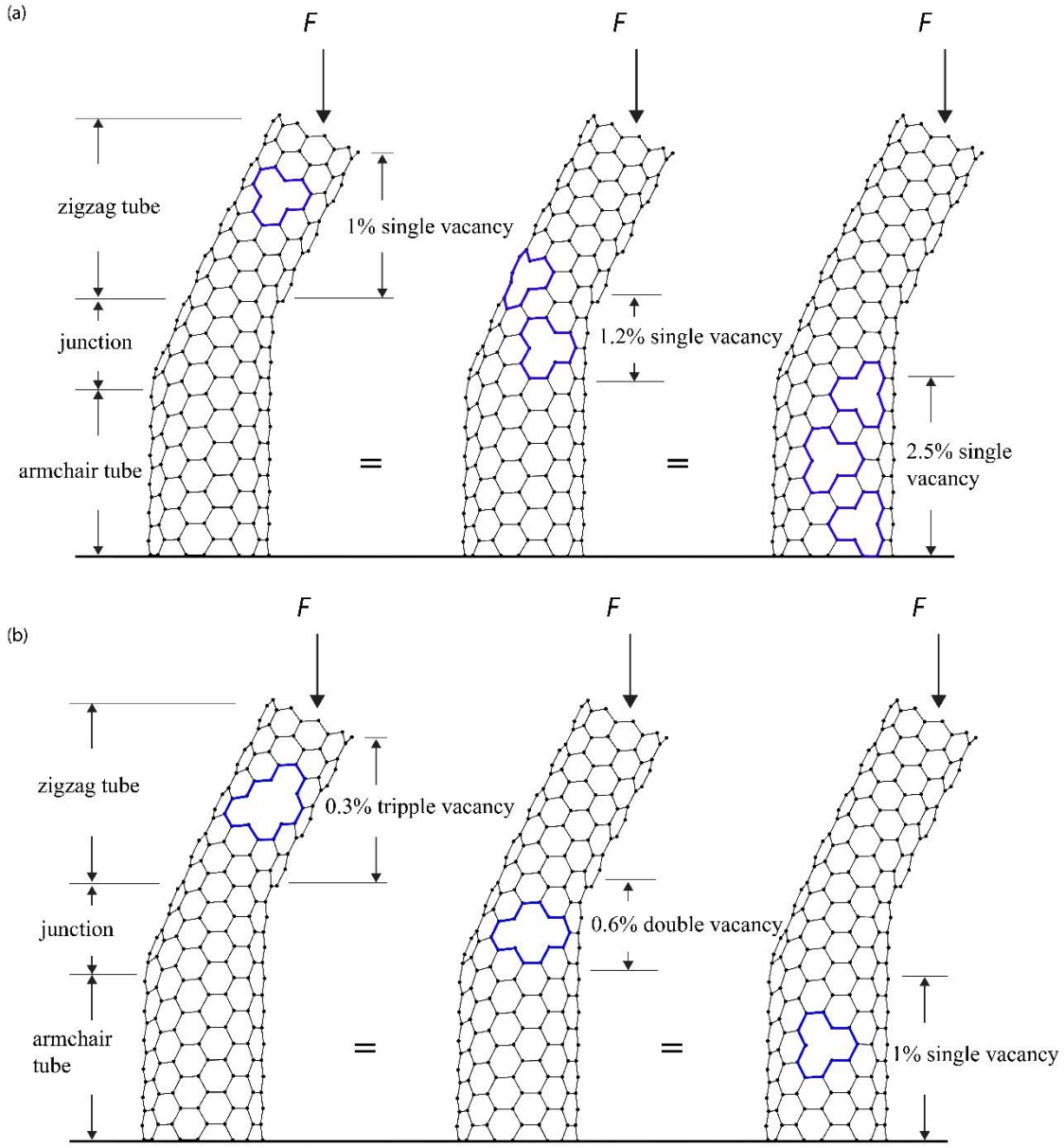

Figure 12. The simulation of buckling analysis of angle-adjoined CNT under the influence of atomic defects.

Considering the obtained values of CBL for different types of nanostructures, it can be concluded that the CBL and as a result, the structural stability of the carbon nanomaterials are determined by their shape, aspect ratio, and the size and location of the vacancies. For the perfect and non-defective models, the overall shape and geometric configuration of the CNT-related material models play a significant role in their structural stability. The CBL values of all models of nanostructures are reduced with the increase of the aspect ratio, which matches the experimental observation that the longer CNTs are easier to be folded [34]. Since the aspect ratio represents the ratio between the length and diameters of the CNTs, the regions with a wider diameter of CNTs, such as the lower regions of nanocone and the wider CNT region in the linearly-joined CNTs, are more stable, which have the same CBL values with higher concentrations of the same type of vacancies in terms to the other regions. At the same time, the stability is also affected by the size of vacancies. The pinhole-vacancy has the greatest impact on the stability. And the presence of mono-vacancy can change the CBL values most slightly in all the considered systems. However, the location of vacancies determined the impact of the vacancy sizes. In the regions with smaller diameter and higher sensitivity to the external forces, the size effect of vacancies is more significant.

Our results also demonstrate that the presence of Stone-Wales defects in the connecting region of hybrid CNTs can reduce their structural stability. From the mechanical aspects, such defects lead to a rearrangement in the harmony of the configuration of the structures. Considering the presence of Stone-Wales defects and the vacancy defects in the junction regions of the CNT hybrids, these joint regions are the critical parts of the linearly-joined and angle-adjoined CNTs, which can significantly influence the overall stability of the carbon nanohybrids.

CONCLUSIONS

In this study, the FEM was employed to understand the impact of different geometric deviations on the buckling properties of carbon nanomaterials. Our CBL value of the homogeneous CNTs matches the previous data obtained from the MD simulation. And the FE analyses on a variety of low-dimensional carbon nanostructures, including nanocone, capped tubes, homogeneous CNTs, linearly-joined and angle-adjoined CNTs, demonstrates that their CBL values are strongly affected by their aspect ratio. The structural stability of all nanostructures reduces with the increase of the aspect ratio, which is also in agreement with the previous MD conclusions. To be more precise, the CBL of nanocone reduces from 50 nN to less than 10 nN when the aspect ratio is changing from 1 to 3. In addition, the CBL of the joint CNT with the wider tube fixed reduces from 70 nN to less than 10 nN when the aspect ratio changes from 5 to 15. The joint CNT with the thinner tube fixed however, keeps moderately reducing its CBL from 5 to almost 1 nN within that phase. The effect of vacancies was also systematically investigated here. And the defects (mono-/bi-/tri-/pinhole vacancies) were introduced to the prefect models at 1.0 % to the total number of atoms in the system. Our results suggest that the CBL values decrease over the size of the vacancies. The pinhole vacancy reveals the highest impact on the stability of the nanostructures, as the reduction of CBL at some stages gets to more than 60% which is a remarkable drop. Since most of the investigated models were structurally asymmetric, the influence of the locations of atomic vacancies on the value of CBL and the structural stability of the nano-configurations was also taken into consideration. The impact of vacancies on the region with large diameters is relatively smaller. Apart from the investigation of the mechanical characteristics of the CNT-related models based on FEM and its particular restrictions, other mechanical approaches such as QM and DFT techniques are strongly advised to evaluate the properties of the nanostructures in a more non-restricted condition, which is currently being investigated by the authors.

Comparing the values of CBL for different material model indicates the fact that the position and the amount of the atomic defects is as highly critical as the geometric configuration of the nanostructures in identifying their mechanical properties, particularly their CBL and structural stability. The presence of atomic defects in any region of a symmetric model may not have a remarkable impact on the CBL when the position of the defect is varied, however, it is essential and critical for asymmetric configurations which are defected by the atomic impurities.

REFERENCES

[1] Dai H, Wong E, Lieber C. Probing electrical transport in nanomaterials: Conductivity of individual carbon nanotubes. Science. 1996;272:523-526.

[2] Saito Y, Hamaguchi K, Hata K. Conical beams from open nanotubes. Nature. 1997; 389:554-555.

[3] Niu C, Sichel EK, Hoch R. High power electrochemical capacitors based on carbon nanotube electrodes. Applied Physics Letters. 1997;70:1480-1482.

[4] Imani Yengejeh S, Kazemi SA, Öchsner A. Advances in mechanical analysis of structurally and atomically modified carbon nanotubes and degenerated nanostructures: A review. Composites Part B: Engineering. 2016;86:95-107.

[5] Gherissi AO. Failure study of the woven composite material: 2.5 D carbon fabric/resin epoxy. Journal of Mechanical Engineering and Sciences. 2019;13:5390-5406.

[6] Ghabezi P, Farahani M. Characterization of cohesive model and bridging laws in mode I and II fracture in nano composite laminates. Journal of Mechanical Engineering and Sciences. 2018;12: 4329-4355.

[7] Xin H, Han Q, Yao XH. Buckling and axially compressive properties of perfect and defective single-walled carbon nanotubes. Carbon. 2007;45:2486-2495.

[8] Li M, Kang Z, Yang P, Meng X, Lu Y. Molecular dynamics study on buckling of single-wall carbon nanotube-based intramolecular junctions and influence factors. Computational Materials Science. 2013;67:390-396..

[9] Imani Yengejeh S, Kazemi SA, Öchsner A. On the buckling behavior of curved carbon nanotubes. Mechanical and materials engineering of modern structure and component design, Springer International Publishing, Switzerland, 2015, 401-412.

[10] Thang PT, Nguyen TT, Lee J. A new approach for nonlinear buckling analysis of imperfect functionally graded carbon nanotube-reinforced composite plates. Composites Part B: Engineering. 2017;127:166-174.

[11] Sangmesh B, Gopalakrishna K, Manjunath S, Kathyayini N, Kadirgama K, Samykano M, Vijayakumar G. Experimental investigation on HSFP using MWCNT based nanofluids for high power light emitting diodes. Journal of Mechanical Engineering and Sciences. 2018;12:3852-3865.

[12] Condon EU, Morse PM. Quantum mechanics of collision processes I. Scattering of particles in a definite force field. Reviews of Modern physics. 1931;3:43.

[13] Ferguson DM, Kollman PA. Can the Lennard–Jones 6-12 function replace the 10-12 form in molecular mechanics calculations?. Journal of computational chemistry. 1991;12:620-626.

[14] Feliciano J, Tang C, Zhang Y, Chen C. Aspect ratio dependent buckling mode transition in single-walled carbon nanotubes under compression. Journal of Applied Physics. 2011;109:084323.

[15] Silvestre N, Wang CM, Zhang YY, Xiang Y. Sanders shell model for buckling of single-walled carbon nanotubes with small aspect ratio. Composite Structures. 2011;93:1683-1691.

[16] Toomsalu E, Koppel IA, Burk P. Critical test of some computational chemistry methods for prediction of gas-phase acidities and basicities. Journal of chemical theory and computation. 2013;9:3947-3958.

[17] Zuberi MJS, Esat V. Investigating the mechanical properties of single walled carbon nanotube reinforced epoxy composite through finite element modelling. Composites Part B: Engineering. 2015;71:1-9.

[18] Imani Yengejeh S, Akbar Zadeh M, Öchsner A. On the tensile behavior of hetero-junction carbon nanotubes. Composites Part B: Engineering. 2015;75:274-280.

[19] Timesli A, Braikat B, Jamal M, Damil N. Prediction of the critical buckling load of multi-walled carbon nanotubes under aial compression. Comptes Rendus Mechanique. 2017;345:158-168.

[20] Nishimura M, Takahashi N, Takagi Y. Relationship between local buckling and atomic elastic stiffness in multi-walled carbon nanotubes under compression and bending deformations. Computational Materials Science. 2017;130:214–221.

[21] Imani Yengejeh S, Öchsner A, Kazemi SA, Rybachuk M. Numerical Analysis of the Structural Stability of Ideal (Defect-Free) and Structurally and Morphologically Degenerated Homogeneous, Linearly-and Angle-Adjoined Nanotubes and Cylindrical Fullerenes Under Axial Loading Using Finite Element Method. International Journal of Applied Mechanics. 2018;10:1850100.

[22] Yao XH, Han Q, Xin H. Bending buckling behaviors of single- and multi-walled carbon nanotubes. Computational Materials Science. 2008;43:579-590.

[23] Hollerer S, Celigoj CC. Buckling analysis of carbon nanotubes by a mixed atomistic and continuum model. Computational Mechanics. 2013;51:765-789.

[24] Imani Yengejeh S, Akbar Zadeh M, Öchsner A. On the buckling behavior of connected carbon nanotubes with parallel longitudinal axes. Applied Physics A. 2014:115:1335-1344.

[25] Li C, Chou TW. A structural mechanics approach for the analysis of carbon nanotubes. International Journal of Solids and Structures. 2003;40:2487–2499.

[26] Kang Z, Li M, Tang Q. Buckling behavior of carbon nanotube-based intramolecular junctions under compression: Molecular dynamics simulation and finite element analysis. Computational Materials Science. 2010;50:253-259.

[27] Sokolnikoff IS. Mathematical theory of elasticity. New York: McGraw-Hill Book Company. 1956.

[28] To CWS. Bending and shear moduli of single-walled carbon nanotubes. Finite Elements in Analysis and Design. 2006;2:404-413..

[29] Kalamkarov AL, Georgiades AV, Rokkam SK, Veedu VP, Ghasemi-Nejhad MN. Analytical and numerical techniques to predict carbon nanotubes properties. International Journal of Solids and Structures. 2006;43:6832–6854.

[30] Song HY, Sun HM, Zhang GX. Molecular dynamic study of effects of Si-doping upon structure and mechanical properties of carbon nanotubes. Communications in Theoretical Physics. 2006;45:741-744.

[31] Ganesan Y, Peng C, Lu Y, Ci L, Srivastava A, Ajayan PM, Lou J. Effect of nitrogen doping on the mechanical properties of carbon nanotubes. ACS nano. 2010;4:7637-7643.

[32] Mehralian F, Tadi Beni Y. Molecular dynamics analysis on axial buckling of functionalized carbon nanotubes in thermal environment. Journal of molecular modeling. 2017;23:330.

[33] Poelma RH, Sadeghian H, Koh S, Zhang GQ. Effects of single vacancy defect position on the stability of carbon nanotubes. Microelectronics Reliability. 2012;52:1279-1284..

[34] Martone A, Faiella G, Antonucci V, Giordano M, Zarrelli M. The effect of the aspect ratio of carbon nanotubes on their effective reinforcement modulus in an epoxy matrix. Composites Science and Technology. 2011;71:1117-1123.